

Inhomogeneity and complexity measures for spatial patterns

R. Piasecki^a, M.T. Martin^b, and A. Plastino^b

^a*Institute of Chemistry, University of Opole, Oleska 48, PL 45052 Opole, Poland*

^b*Argentina National Research Council (CONICET) and
National University La Plata, C.C. 727, (1900) La Plata, Argentina*

Abstract

In this work we examine two different measures for inhomogeneity and complexity that are derived from non-extensive considerations à la Tsallis. Their performance is then tested on theoretically generated patterns. All measures are found to exhibit a most sensitive behaviour for Sierpinski carpets. The procedures here introduced provide us with new, powerful Tsallis' tools for analysing the inhomogeneity and complexity of spatial patterns.

PACS. 05.90.+m **KEYWORDS:** Non-extensive statistics, complexity, spatial patterns.

1. Introduction

In spite of its great success, the statistical mechanics paradigm based on the Boltzmann-Gibbs entropic measure seems to be inadequate to deal with many interesting physical scenarios [1,2,3]. Astronomical self-gravitating systems constitute an important illustrative example of these difficulties [4].

In this paper we are concerned with measures of spatial inhomogeneity and complexity for different length scales. A recent study [5] has advanced a quantitative characterization of morphological features of a material system. This characterization is based upon a normalized information (entropic) measure, more general than both i) the so-called local porosity entropy [6] and ii) the “configuration entropy” [7], two concepts that have been shown to be connected in [8]. Here we wish to introduce Tsallis' generalized measures into this area of endeavor. We will show that they provide us with a quite useful research tool that allows for fruitful insights concerning both inhomogeneity and complexity of spatial patterns.

2. Entropic measures

2.1 Recapitulation of the microcanonical formalism and of the averaging procedure

We deal here mainly with the two information measures i) S_Δ and ii) $S_\Delta(\text{PO})$. The first refers to finite-sized objects (FSOs) and is fully described in [9]. The second one, for the simpler case of “point” objects (POs), was used in [10,11] under a different notation (“ $f(S)$ ”). The method of [9] is exact when applied to the evaluation of the spatial inhomogeneity of identical FSOs (at different length scales). The latter one [10,11] can be regarded as exact for investigating the degree of inhomogeneity in a phase space.

Consider a mixture of non-interacting and of equal size (1×1 in pixels) black and white objects (it should be noticed that, arguably, these “particles” interact with each other through mutual exclusion). We talk of, respectively, black and white pixels. For a given $L \times L$ grid, let us have n black pixels ($0 < n < L^2$) pixels and $m = L^2 - n$ white pixels, distributed in square, non-overlapping and distinguishable $\chi = (L/k)^2$ lattice cells of size $k \times k$ (no pores). For each length scale k we assume standard constraints for the cell occupation numbers, i.e., $n_1 + n_2 + \dots + n_{\chi(k)} = n$, and, correspondingly, $m_1 + m_2 + \dots + m_{\chi(k)} = m$, with $m_i(k) + n_i(k) = k^2$ for $i = 1, 2, \dots, \chi(k)$.

Consider all distributions of these objects with fixed occupation numbers as a kind of scale-dependent configurational *macrostate*, described by the set $\{n_i(k)\} \equiv \{n_1, n_2, \dots, n_{\chi(k)}\}$ (for black pixels). A corresponding macrostate for white pixels $\{k^2 - n_1, k^2 - n_2, \dots, k^2 - n_{\chi(k)}\}$ is automatically at hand. We can limit ourselves to a black pixels' language. For a given length scale k , any macrostate can be realized by a number of distinguishable arrangements of n black pixels associated with the 1×1 lattice cells, i.e., a kind of “equally likely” configurational

microstates, with $n_i = 0$ or 1. Setting the Boltzmann constant $k_B = 1$ we use the standard definition of configurational (Boltzmann micro-canonical) entropy

$$S(k) = \ln \Omega(k) \equiv \ln \left[\prod_{i=1}^{\chi} \binom{k^2}{n_i} \right], \quad (1)$$

where $\Omega(k)$ is the total number of distinguishable spatial arrangements of the objects in $\chi(k)$ cells of size $k \times k$, each containing $n_i(k)$ black pixels and $m_i(k)$ white pixels.

The number of distinguishable spatial arrangements of our objects increases when they are mixed. For every length scale $1 < k < L$, there is a *special set* of the “most spatially ordered” object-distributions containing $\Omega_{\max}(k)$ configurations. These are distinguished by the condition $|n_i(k) - n_j(k)| \leq 1$ (holding for each pair $i \neq j$). Every configuration belonging to such a *special set* represents a *reference configurational macrostate* $\{n_i(k)\}_{\text{RCM}}$ having the highest possible value of configurational entropy $S_{\max}(k)$. On the other hand, for $k = 1$ and for $k = L$ we have always $S_{\max}(1) = S(1) = 0$ and $S_{\max}(L) = S(L) \neq 0$. In general, for a given $\{n_i(k)\}_{\text{RCM}}$

$$S_{\max}(k) = \ln \Omega_{\max}(k) \equiv \ln \left[\binom{k^2}{n_0}^{\chi - n_0} \binom{k^2}{n_0 + 1}^{n_0} \right], \quad (2)$$

with $r_0 = n \bmod \chi$, $r_0 \in \{0, 1, \dots, \chi - 1\}$, and $n_0 = (n - r_0)/\chi$, $n_0 \in \{0, 1, \dots, k^2 - 1\}$.

We shall concentrate our efforts on ascertaining the dependence of the spatial inhomogeneity of the mixture on the length scale k by using an information measure to be defined below. In order to evaluate, for each k , the deviation of the macrostate $\{n_i(k)\}$ represented by an actual configuration from the appropriate $\{n_i(k)\}_{\text{RCM}}$ one it is natural to consider the difference $S_{\max}(k) - S(k)$. Averaging this difference over the number of cells $\chi(k)$ we obtain a relative measure (per cell) of the spatial inhomogeneity of our mixture

$$S_{\Delta}(k) = \frac{S_{\max} - S}{\chi} \equiv \frac{r_0}{\chi} \ln \left(\frac{k^2 - n_0}{n_0 + 1} \right) + \frac{1}{\chi} \sum_{i=1}^{\chi} \ln \left[\binom{k^2}{n_i} / \binom{k^2}{n_0} \right]. \quad (3)$$

This averaging procedure is necessary for the validity of a crucial measure’s property that allows for its calculation at every length scale (see Appendix A). According to this definition, every binary pattern can be treated as spatially homogeneous at length scales $k = 1$ and $k = L$.

In recent studies [12,13] a measure of “complexity” was considered that can be expressed in terms of order/disorder. Adapted to our spatial case, the simplest form of this measure can be written as

$$\Gamma(k) = \begin{cases} 0 & \text{for } k = 1, L \\ \Delta (1 - \Delta) & \text{for } 1 < k < L \end{cases} \quad (4)$$

where $\Delta \equiv S(k)/S_{\max}(k)$. Notice that this “length-scale dependent” form differs from the original one given in [13] (see also [14]). There is a clear correlation between $S_{\Delta}(k)/k^2$, on the one hand, and $\Gamma(k)$ on the other one (see Figs. 1a, b). Remaining traces of small discrepancy at $k = 3$, as we shall see later on with reference to Fig 4a, will be also present in the q -dependent behaviour of $\Gamma_q(k = 3)$. The two binary patterns depicted in the insets of Figs. 1a,b are used for testing purposes. For a deterministic Sierpinski carpet [9] the notation $\text{DSC}(a,b,c)$ refers to an initial square lattice of $L \times L$ cells, with $L = a^c$, divided into a^2 sub-squares, with only b of them conserved according to a deterministic rule. Such a decimation procedure is repeated on each conserved sub-square, and so on, c times. The second pattern refers to a low structured random arrangement (called an R pattern) of the same numbers $n = 512$ (black) and $m = 217$ (white) pixels, as, for instance, $\text{DSC}(3,8,3)$.

2.2. Extension of the formalism to a generalised setting and examples

Focus attention now upon Tsallis generalised information measure [1]. It is easy to see that

$$S_q = \frac{\text{const. factor}}{q-1} \left[1 - \sum_{i=1}^W p_i^q \right] \xrightarrow{\text{foreach } i \text{ } \lim p_i = 1/W} \frac{W^{1-q} - 1}{1-q} \xrightarrow{\lim q = 1} \ln W, \quad (5a)$$

or

$$S_q = \frac{\text{const. factor}}{q-1} \left[1 - \sum_{i=1}^W p_i^q \right] \xrightarrow{\lim_{q \rightarrow 1}} - \sum_{i=1}^W p_i \ln p_i \xrightarrow[\text{for each } i]{\lim_{p_i = 1/W}} \ln W, \quad (5b)$$

where W is the total number of possible microstates ($W \equiv \Omega$ in our notation for configurational microstates), $\{p_i\}$ the associated probabilities, and q the *non-extensivity* (real) parameter. For convenience, the constant Boltzmann's factor is set equal to unity.

At this point our investigation begins. We ask now *whether there exists a well-defined q -extension of the information measure given by Eq. (3).* We require also that it should retain the above referred to crucial property, *i.e.*, the one that allows for calculating the measure at every length scale (see Appendix A). What motivates this type of generalisation is the expectation that the strong nonlinearity of the measure will reveal new features regarding POs and FSOs. Notice that we can use (in the reverse direction) each of the middle expressions of (5a) and (5b).

2.2.1 A-approach

Let us denote as **(A)** the (5a)-approach. Considering the appropriate equally likely configurational microstates (with $n_i = 0$ or 1) for a given macrostate, for both i) $p_i(k) = 1/\Omega(k)$ and ii) the ‘‘reference macrostate’’ $p_{i, \max}(k) = 1/\Omega_{\max}(k)$, we obtain in natural fashion

$$S_q(k; \mathbf{A}) = \frac{\Omega(k)^{1-q} - 1}{1-q}, \quad S_{q, \max}(k; \mathbf{A}) = \frac{\Omega_{\max}(k)^{1-q} - 1}{1-q}, \quad (6a,b)$$

and

$$S_{\Delta, q}(k; \mathbf{A}) = \frac{1}{\chi} \frac{\Omega_{\max}(k)^{1-q} - \Omega(k)^{1-q}}{1-q}. \quad (7)$$

A word of caution is needed here. For a fixed configurational macrostate $\{n_i(k=1)\}$ there is only one proper microstate and $\Omega(1) = \Omega_{\max}(1) = 1$. In turn, for a given $\{n_i(k=L)\}$ we have $\Omega(L) = \Omega_{\max}(L) \neq 0$. Thus, for both limit cases we have $S_{\Delta, q}(k=1 \text{ or } L; \mathbf{A}) \equiv 0$, as expected. However, for any configurational macrostate $\{n_i(1 < k < L)\}$, Tsallis' measure depends on the number of cells $\chi(k)$ in such a way that results for the constant cell number, $\chi = (kL/k)^2 \equiv L^2$ will differ from those for the optimal one. More to the point, for $IL \bmod k = 0$ we have $\chi = (IL/k)^2$ in contrast to what happens with the behaviour of the measure $S_{\Delta}(k)$ given by Eq. (3). This situation is illustrated in Fig. 2. In both cases the curves corresponding to $q > 1$ ($q < 1$) converge to the case $q = 1$ from opposite sides.

An interesting fact is to be pointed out here: $S_{\Delta, q}$ exhibits the same features (upper curves for $q < 1$ and bottom ones for $q > 1$) displayed, with reference to the case $q = 1$ (see Fig. 1 of [15]), by the Kolmogorov-Sinai-Tsallis entropy (evaluated numerically). The 1D window of length N referred as *time* in [15] corresponds to our length scale k .

2.2.2 B-approach

Let us denote as **(B)** the (second) approach that employs Eq. (5b). Introducing a *local* black pixels fraction $\gamma_i(k) = n_i/k^2$ for the i th cell of size $k \times k$, and the corresponding fraction for white pixels (namely, $1 - \gamma_i(k)$), the Shannon-like forms $S(k)$ and $S_{\max}(k)$ can be recast, using the Stirling approximation $\ln n! \sim n \ln n - n$, in the fashion

$$S(k; \mathbf{B}) \equiv -k^2 \sum_{i=1}^{\chi} [\gamma_i \ln \gamma_i + (1 - \gamma_i) \ln (1 - \gamma_i)] \equiv k^2 \sum_{i=1}^{\chi} S_i(\gamma), \quad (8a)$$

$$\begin{aligned} S_{\max}(k; \mathbf{B}) &\equiv -k^2(\chi - r_0) [\varphi_0 \ln \varphi_0 + (1 - \varphi_0) \ln (1 - \varphi_0)] - k^2 r_0 [\varphi_1 \ln \varphi_1 + (1 - \varphi_1) \ln (1 - \varphi_1)] \\ &\equiv k^2(\chi - r_0) S_0 + k^2 r_0 S_1 \end{aligned} \quad (8b)$$

and finally,

$$S_{\Delta}(k; \mathbf{B}) = \frac{k^2}{\chi} \left[(\chi - r_0) S_0 + r_0 S_1 - \sum_{i=1}^{\chi} S_i(\gamma) \right], \quad (9)$$

where $\varphi_0 = n_0/k^2$ and $\varphi_1 = (n_0 + 1)/k^2$. We immediately recognise as familiar the forms $S_i(\gamma)$, S_0 , and S_1 . They are ‘‘local’’ entropies. The very small differences between these Shannon-like measures and the Boltzmann ones given

by Eq. (3) appear only at the smaller length scales. The corresponding curves are practically indistinguishable at our drawings' scale.

We can now generalise as above and obtain $S_q(k; \mathbf{B})$ by recourse to the Jackson's q -derivative [16] $D_q f(x) \equiv [f(qx) - f(x)]/[qx - x]$ (see, for instance, the work of Abe [17]). This derivative ascertains just how the function $f(x)$ "reacts" under dilatation of the x coordinate, opening thus a wide door for getting thermodynamical insights [18]. Within the framework of such an approach the normalisation identity $\sum_{i=1}^W p_i \equiv 1$ is not really needed. This fact might have some possible bearings on the so-called incomplete normalisation for microcanonical ensembles [19].

We can apply the Jackson derivative to each pair of local concentrations, as for instance

$$-D_q [\gamma_i^x + (1-\gamma_i)^x] \Big|_{x=1} = \frac{1 - [\gamma_i^q + (1-\gamma_i)^q]}{q-1}, \quad (10)$$

thus getting

$$S_q(k; \mathbf{B}) = k^2 \sum_{i=1}^Z \left\{ \frac{1 - [\gamma_i^q + (1-\gamma_i)^q]}{q-1} \right\} \equiv k^2 \sum_{i=1}^Z S_{i,q}(\gamma). \quad (11a)$$

Note that the appropriate expression for the configurational entropy of a mixture of black and white pixels, for a given length scale, is now obtained in terms of i) the total number of cells and ii) the local pixel fractions, *not in terms of W and p_i* . In a similar vein we find

$$\begin{aligned} S_{q,\max}(k; \mathbf{B}) &= k^2 \left\{ (\chi - r_0) \frac{1 - [\varphi_0^q + (1-\varphi_0)^q]}{q-1} + r_0 \frac{1 - [\varphi_1^q + (1-\varphi_1)^q]}{q-1} \right\} \\ &\equiv k^2 [\chi - r_0] S_{0,q} + r_0 S_{1,q} \end{aligned} \quad (11b)$$

and finally,

$$S_{\Delta,q}(k; \mathbf{B}) = \frac{k^2}{\chi} \left[(\chi - r_0) S_{0,q} + r_0 S_{1,q} - \sum_{i=1}^Z S_{i,q}(\gamma) \right]. \quad (12)$$

For q close to 1 the correctness of above formulae was confirmed by using a Taylor expansion up to order four in the difference (Jackson) operator [20]. Fig. 3a depicts the typical behaviour of $S_{\Delta,q}(k; \mathbf{B})$ versus length scale k for i) two different q -parameters and ii) for their associated inverse values $1/q$. Both the DSC(3,8,3) and the R patterns are here considered. The Tsallis form $S_{\Delta,q}(k; \mathbf{B})$ reduces to the corresponding Shannon one $S_{\Delta}(k; \mathbf{B})$ for $q \rightarrow 1$. For the sake of completeness we also give here the final formula for the PO-measure (Appendix B). In the case of the \mathbf{B} approach it reads

$$S_{\Delta,q}(k; \text{PO}, \mathbf{B}) = \frac{n}{\chi(q-1)} \left[-(\chi - r_0)(n_0/n)^q - r_0((n_0+1)/n)^q + \sum_{i=1}^Z (n_i/n)^q \right]. \quad (13)$$

The measure (13) exhibits a similar dependence on the number of cells $\chi(k)$, (either constant or optimal) as the measure given by Eq. (7). For the latter one this seems quite natural, since the measure $S_{\Delta,q}(k; \mathbf{A})$ *a priori* "neglects" any correlations between the p_i . On the other hand, the measure $S_{\Delta,q}(k; \text{PO}, \mathbf{B})$ does not take into account the additional, length-scale dependent constraints for FSOs (like $n_i \leq k^2$), in contrast to what happens with the restricted local fractions $\gamma_i(k)$ and $1 - \gamma_i(k)$ incorporated into the measure $S_{\Delta,q}(k; \mathbf{B})$. Mathematically, these differences manifest themselves i) in a global normalisation of the POs fractions, *i.e.*, $\sum_{i=1}^Z (n_i/n) \equiv 1$, and ii) in a local one for FSOs fractions, $\gamma_i(k) + 1 - \gamma_i(k) \equiv 1$. Notice that only in the latter case, considered globally, we have $\sum_{i=1}^Z [\gamma_i + (1 - \gamma_i)] \equiv \chi$, as required in order that the "external" averaging (by the total number of cells $\chi(k)$) will remain effective.

The above feature of $S_{\Delta,q}(k; \text{PO}, \mathbf{B})$ forces us to use it just for a constant number of cells. Fig. 3b depicts the typical behaviour of $S_{\Delta,q}(k; \text{PO}, \mathbf{B})$, versus the length scale k , for a given q -parameter and also for its associated $1/q$ -value, for both the DSC(3,8,3) and the R patterns. Notice that the behaviour displayed in Fig. 3b is quite different from that for FSOs in Fig. 3a. Also, the measure used in Fig. 3b is not symmetrical with respect to black and white pixels, as is the case for FSO-measures. We point out that the patterns investigated here are biased ones from the viewpoint of PO-measures: we have black pixel (not point) occupation numbers for a binary image, and n_i

never exceeds k^2 . We should remember that all “true” point-objects can be placed into one (and the same) cell, independently of the cell’s size.

2.2.3 Non-extensivity and differences between finite size and point objects

We are now in a position to investigate (at chosen length scales) the q -differences between FSOs and POs by recourse to $S_{\Delta, q}(k; \mathbf{B})$, $S_{\Delta, q}(k; \text{PO}, \mathbf{B})$, on the one hand, and also to $\Gamma_q(k; \mathbf{B})$ and $\Gamma_q(k; \text{PO}, \mathbf{B})$, on the other one. The last two measures come from Eq. (4), where we replaced (in Δ) the appropriate entropies with the new ones of Eqs. (11a,b) and (B5,B6), respectively. Only for the DSC (the more interesting instance from the complexity view point) will we examine the behaviour for both FSOs and POs. Let us concentrate on the q -dependence around $q = 1$, the most interesting region from a physical viewpoint. In the case of FSOs we can observe, in Fig. 4a, a maximum of spatial complexity (solid lines) at $k = 3$ (for $q < 1$), while at the other scales (k -values) we see a different behaviour for both $\Gamma_q(k; \mathbf{B})$ (solid lines) and $\Gamma_q(k; \text{PO}, \mathbf{B})$ (dashed lines), as we pass from the $q < 1$ - to $q > 1$ -region. The selected k -values, $k = 3, 9, 6$. and 18 , correspond to the decreasing, sequential succession of pronounced peaks in Fig. 1a.

These differences between the FSOs and POs can still be seen in Figs. 4b,c. The two measures $S_{\Delta, q}(k; \mathbf{B})$ (for $k \geq 3$) and $S_{\Delta, q}(k; \text{PO}, \mathbf{B})$ (for $k \geq 8$ except $k = 9$) exhibit a non-monotonous behaviour. Again, the chosen scales correspond to the decreasing succession of well-marked peaks in Fig. 3a. The PO-measure exhibits a peak of spatial inhomogeneity for $q = 0.151, 0.150, 0.152$ at the length scales $k = 18, 15, 21$. For $k = 9$, the value of the measure grows in monotonic fashion as $q \rightarrow 0^+$ (see Fig. 4c). In Fig. 4b we dropped off this region so as to better depict the q -dependent position of the FSO-measure’s maximum. The FSO-measure exhibits peaks at the q -values: $1.052, 1.096 \pm 7, 1.030 \pm 1$ for $k = 18, 15, 21$. Notice also the peak, for $k = 9$, at $q = 0.770 \pm 1$, absent in the PO-instance, which does not diminish as $q \rightarrow 0^+$ (at this scale we can have $n_i = 0$, which is not possible for larger scales). The associated maxima are significantly larger than those corresponding to Shannon’s entropy (horizontal lines) for the FSO- (PO-measure). Note that in a recent study, Johal [21], instead of using the difference $S_{\max} - S$ per cell, as we do here, considers just the entropy S itself. Moreover, a different “ q -modification” of the Shannon’s and Tsallis forms was introduced. Their results are similar to ours for q -values in the vicinity of $q = 1$, in the case of POs.

The q -dependence investigated here allows for an additional interesting observation, related to FSO- and PO-measures of spatial inhomogeneity. *At each scale, the two concomitant curves coincide for a finite and non-zero value of q , say, $q^*(k)$.* This means that for such a value of q , any geometrical constraint connected with the FSOs is somehow “translated” into the PO description. Thus, *each FSO can be treated as a PO*, which quite agrees with an intuitive picture of no-extensivity. Note that such a feature is absent in the case of the complexity measures investigated in this paper.

A still open question is related to the physical meaning of the entropic index q for binary patterns. Recently [22-24], a meaningful relation between q and the relative variance of locally fluctuating variables has been encountered, provided the fluctuating parameter is χ^2 distributed. Given a binary pattern, the occupation numbers are distributed around the average number per cell. The deviation from the average depends on the structure. For instance, the relative variance is higher for a DSC than for the corresponding R pattern. Thus, if the occupation numbers are properly distributed, we can formally associate a q -parameter to such a pattern. This approach (although quite formal) may shed some light on the scale dependent structural properties of binary patterns.

3. Conclusions

Our first remark concerns the nature of the approaches **A** and **B**. The **B**-technique seems to be more adequate for our purposes *because it is cell independent*. For this reason, method **B** was the one employed to compare i) length scale’s differences and ii) q -differences between point objects and finite size ones.

For point (finite size) objects we detect a qualitative (quantitative indeed, for larger k -values) similarity, at different length scales, between $1/q$ and q -results (see Figs. 3a,b). With regards to the q -differences between point objects and finite size ones, let us focus out attention upon the most interesting interval, namely, $0 < q < 2$. The spatial complexity of POs (FSOs) decreases with q , while the corresponding degree of spatial inhomogeneity, in both cases, is of a non-monotonous nature (see Figs. 4a and 4b,c), with the exception of a few length scales for POs and of the length $k = 2$ for FSOs.

The cell dependence detected with the method **A** (see Eqs. (6,7)) strongly suggests that the only valid micro-canonical expression is the logarithmic one of Boltzmann’s. Using instead the so-called \ln_q does not reproduce the correct micro-canonical results.

Appendix A

The following property allows us to calculate the value of a measure at *every* length scale, i.e. for $k=1, 2, 3, \dots, L$. If a final pattern of size $lL \times lL$ (where l is a natural number) is formed by the periodic repetition of an initial arrangement of size $L \times L$, then the value of the measure at a given length scale $1 \leq k \leq L$ commensurate with the side length L is *unchanged* under the replacement $L \leftrightarrow lL$, since it also causes $n \leftrightarrow l^2 n$, $\chi \leftrightarrow l^2 \chi$, $r_0 \leftrightarrow l^2 r_0$, keeping unchanged both n_0 and the corresponding n_i . To overcome the problem of an incommensurate length scale it is sufficient to determine a number l such that $lL \bmod k = 0$ and replace the initial arrangement of size $L \times L$ by the periodically created one of size $lL \times lL$. We define then $S_\Delta(k, L, n) \equiv S_\Delta(k, lL, l^2 n)$.

Appendix B

For the PO-measure [10], that takes into consideration the black pixels as ‘‘points’’ (n_i per cell) while the white pixels are treated as a continuous medium, appropriate Shannon-like forms are given by

$$S(k; \text{PO}) = \ln \left\{ \frac{n!}{n_1! n_2! \dots n_\chi!} \right\} \cong -n \sum_{i=1}^{\chi} (n_i/n) \ln(n_i/n) , \quad (\text{B1})$$

$$S_{\max}(k; \text{PO}) = \ln \left\{ \frac{n!}{(\chi - r_0) n_0! r_0 (n_0 + 1)!} \right\} \cong -n [(\chi - r_0)(n_0/n) \ln(n_0/n) + r_0 ((n_0 + 1)/n) \ln((n_0 + 1)/n)] \quad (\text{B2})$$

and

$$S_\Delta(k; \text{PO}) = \frac{S_{\max}(k; \text{PO}) - S(k; \text{PO})}{\chi} \quad (\text{B3})$$

with n_0 and r_0 defined above. The associated Tsallis-like forms referred to as ‘‘the (B) approach’’ can be obtained by using again the Jackson derivative for each local cell

$$-D_q (n_i/n)^x \Big|_{x=1} = [(n_i/n) - (n_i/n)^q] / (q-1) , \quad (\text{B4})$$

yielding

$$S_q(k; \text{PO}, \mathbf{B}) = n \left[1 - \sum_{i=1}^{\chi} (n_i/n)^q \right] / (q-1) \quad (\text{B5})$$

and

$$S_{q, \max}(k; \text{PO}, \mathbf{B}) = n \left[1 - (\chi - r_0)(n_0/n)^q - r_0 ((n_0 + 1)/n)^q \right] / (q-1) . \quad (\text{B6})$$

The (not used here) Tsallis-like forms for POs corresponding to the (A) approach can be obtained following the steps leading to Eqs. (6, 7), and using the proper number of possible micro-states described in (B1) and (B2).

References

- [1] C. Tsallis, J. Stat. Phys. 52, (1988) 479; Physica A 221 (1995) 277; Braz. J. Phys. 29 (1999) 1.
- [2] C. Tsallis, Chaos, Solitons, and Fractals 6 (1995) 539, and references therein.
- [3] A. Plastino and A.R. Plastino, Braz. J. Phys. 29 (1999) 50; Phys. Lett. A177 (1993) 177.
- [4] A.R. Plastino and A. Plastino, in Condensed Matter Theories, Volume 11, E. Ludena (Ed.), Nova Science Publishers, New York, USA, (1996) p. 341; Phys. Lett. A 174 (1993) 384; Braz. J. Phys. 29 (1999) 79.
- [5] C. De W. Van Siclen, Phys. Rev. E 56 (1997) 5211.
- [6] F. Boger, J. Feder, T. Jossang, and R. Hilfer, Physica A 187 (1992) 55.
- [7] C. Andraud, A. Beghdadi, and J. Lafait, Physica A 207 (1994) 208.
- [8] C. Andraud, A. Beghdadi, E. Haslund, R. Hilfer, J. Lafait, and B. Virgin, Physica A 235 (1997) 307.
- [9] R. Piasecki, Physica A 277 (2000) 157; Surf. Sci. 454-456 (2000) 1058.
- [10] Z. Garncarek, R. Piasecki, Eur. Phys. J. Appl. Phys. 5 (1999) 243.
- [11] Z. Garncarek, T. Majcherczyk, D. Potoczna-Petru, and R. Piasecki, J. Mater. Sci. Lett. 19 (2000) 1369.
- [12] J.S. Shiner and P.T. Landsberg, Phys. Lett. A 245 (1998) 228.
- [13] J.S. Shiner, M. Davison, and P.T. Landsberg, Phys. Rev. E 59 (1999) 1459.
- [14] J. P. Crutchfield and D.P. Feldman, cond-mat/0102181, and references therein.

- [15] M.Buiatti , P. Grigolini and L. Palatella, Physica A 268 (1999) 214.
- [16] F. Jackson, Mess. Math. 38 (1909) 57; Quart. J. Pure Appl. Math. 41 (1910) 193.
- [17] S. Abe, Phys. Lett. A 224 (1997) 326.
- [18] C. Tsallis, cond-mat/0010150.
- [19] Q. A. Wang, Chaos, Solitons and Fractals 12 (2001) 1431, cond-mat/0107065.
- [20] H.-y. Pan, Z.S. Zhao, Phys. Letters A 282 (2001) 251.
- [21] R.S. Johal, Phys. Rev. E 58 (1998) 4147.
- [22] G. Wilk and Z. Włodarczyk, Phys. Rev. Lett. 84 (2000) 2770.
- [23] G. Wilk and Z. Włodarczyk, hep-ph/0004250.
- [24] C. Beck, cond-mat/0105058 and 0105371.

Figure caption

Fig. 1. $S_{\Delta}(k)/k^2$ –measure (solid line) and the complexity measure $\Gamma(k)$ (dashed line) are plotted as a function of the length scale for the binary patterns depicted in the insets. The correlation between the two measures is also shown in the insets: full circles correspond to the $\Gamma(k)/S_{\Delta}(k)$ ratio, while the solid line depicts the $1/k^2$ function. (**Fig. 1a**) DSC(3,8,3) pattern and (**Fig. 1b**) R pattern.

Fig. 2. Entropic q -measure (Cf. Eq. (7), **A** approach) for FSOs, as a function of the length scale, for a constant number of cells (in the insets, for an optimal number of cells). Short dashed lines (bottom for q and upper for $1/q$) correspond to $q = 1.00001$, while long dashed lines (bottom (q) and upper ($1/q$)) are drawn for $q = 1.000005$. We depict also the corresponding Boltzmann’s measure (Cf. Eq. (3)) for $q = 1$ (solid line). (**Fig. 2a**) DSC(3,8,3) and (**Fig. 2b**) R pattern.

Fig. 3. Entropic q -measure in the **B** approach, as a function of the length scale for the DSC pattern (in the insets, for the R pattern). We depict also the corresponding Shannon’s measure for $q = 1$: full circles, according to Eq. (9), and open ones according to Eq. (B3). (**Fig. 3a**) for FSOs (Cf. Eq. (12)), with $q = 2.5$ and 5 , from top to bottom, respectively (solid lines). The associated $1/q$ counterparts are represented by dashed lines. (**Fig. 3b**) for POs (Cf. Eq. (13)) with a constant number of cells and $q = 1.1$ (solid line), and $1/q$ counterpart (dashed line).

Fig. 4. FSO- and PO-measures, **B** approach, as a function of the q parameter at fixed length scales for the DSC pattern. (**Fig. 4a**) the complexity measure $\Gamma_q(\mathbf{B})$ for FSOs (from the top: $k = 3, 9, 6, 18$ (solid lines), and, similarly, $\Gamma_q(\text{PO}, \mathbf{B})$ for POs (dashed lines). Note that at scale $k = 6$ the spatial complexity is lower than at $k = 9$, in agreement with the results of Figure 1a. (**Fig. 4b**) the inhomogeneity measure $S_{\Delta, q}(\mathbf{B})$ for FSOs (from the top: thick ($k = 9$), dot-dashed ($k = 18$), solid ($k = 15$), and dashed ($k = 21$)). Same for the $S_{\Delta, q}(\text{PO}, \mathbf{B})$. (**Fig. 4c**) the inhomogeneity measure $S_{\Delta, q}(\text{PO}, \mathbf{B})$. Remaining details are as in Fig. 4b. For the sake of clarity, the corresponding Shannon’s values (horizontal lines) are drawn for FSOs only. Note that at scale $k = 15$, the spatial inhomogeneity is lower than at $k = 18$, in agreement with the results of Figure 3a.

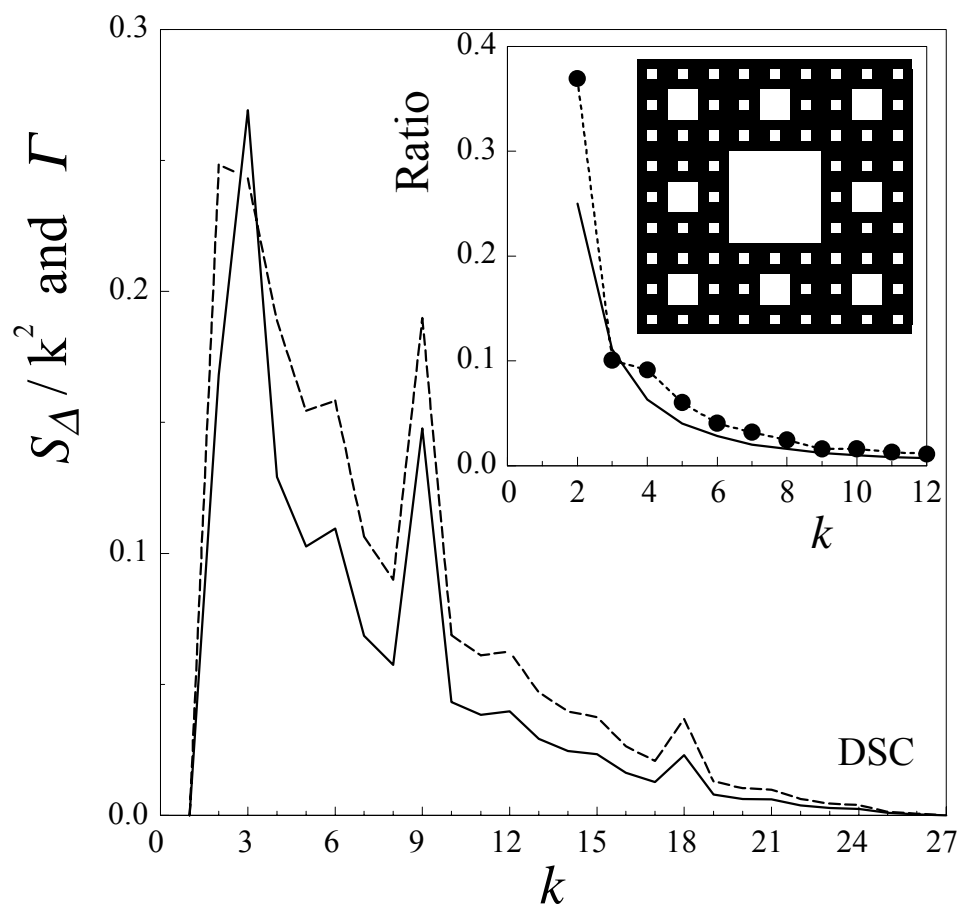


Fig. 1a

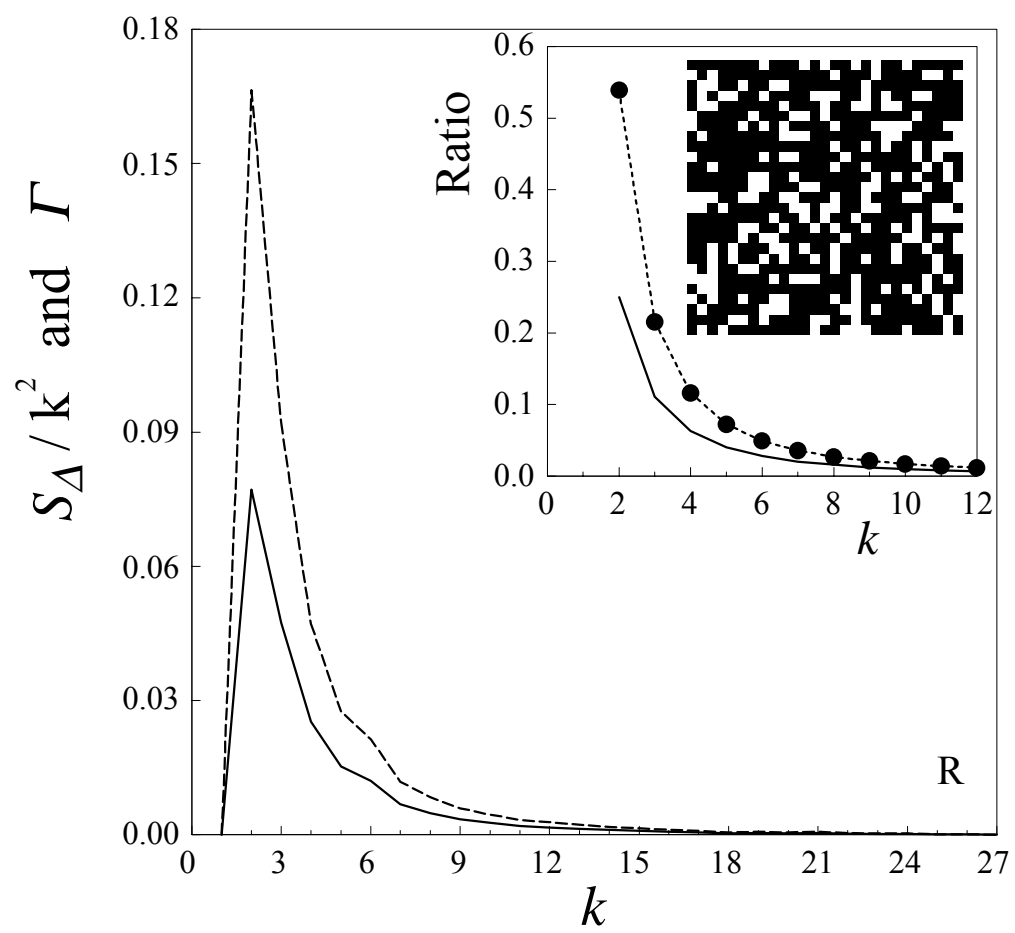


Fig. 1b

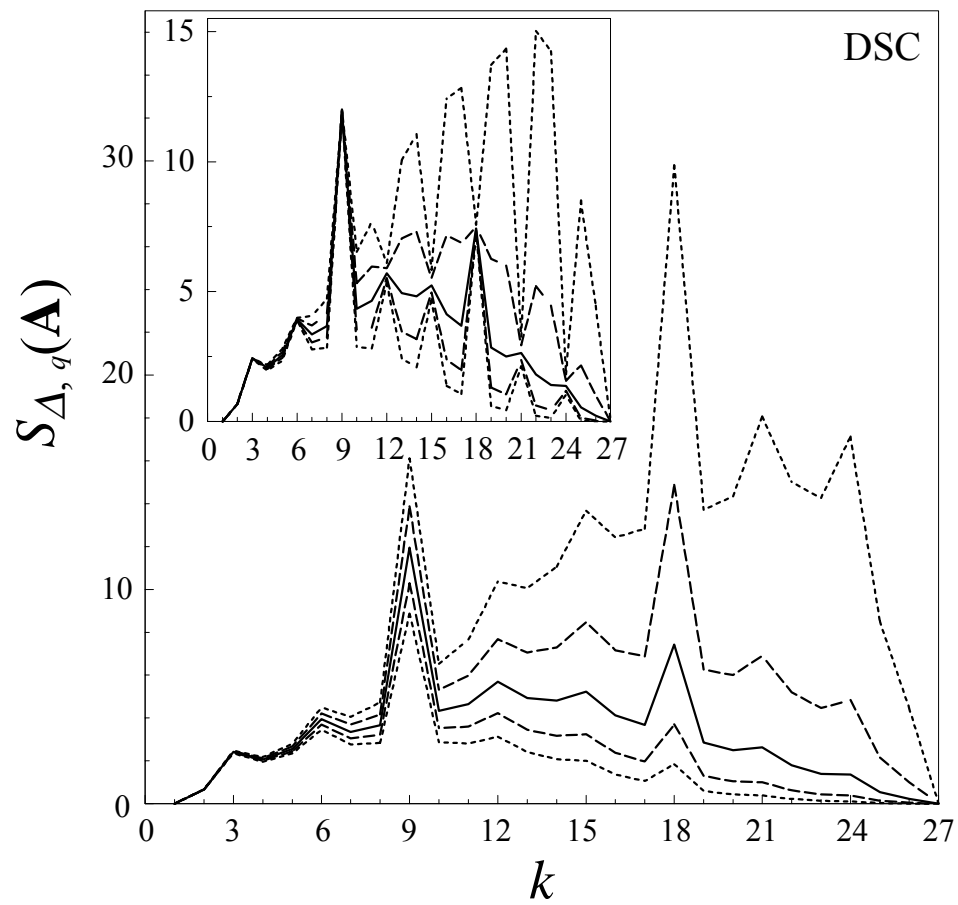


Fig. 2a

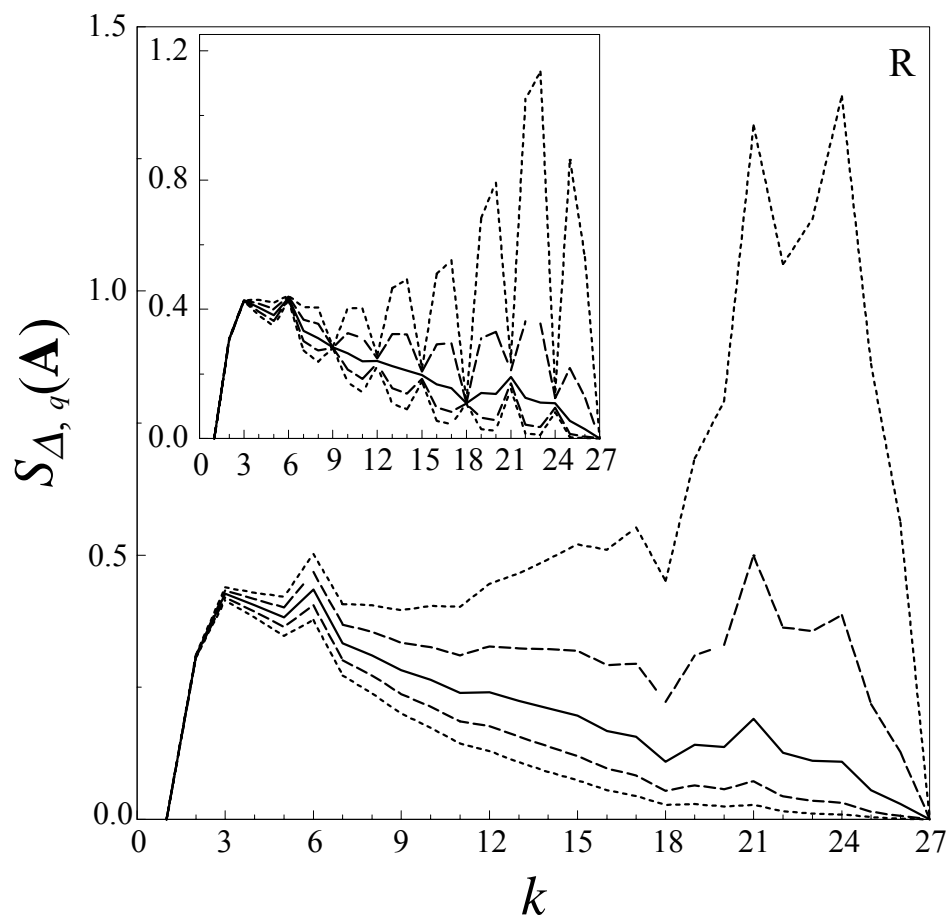


Fig. 2b

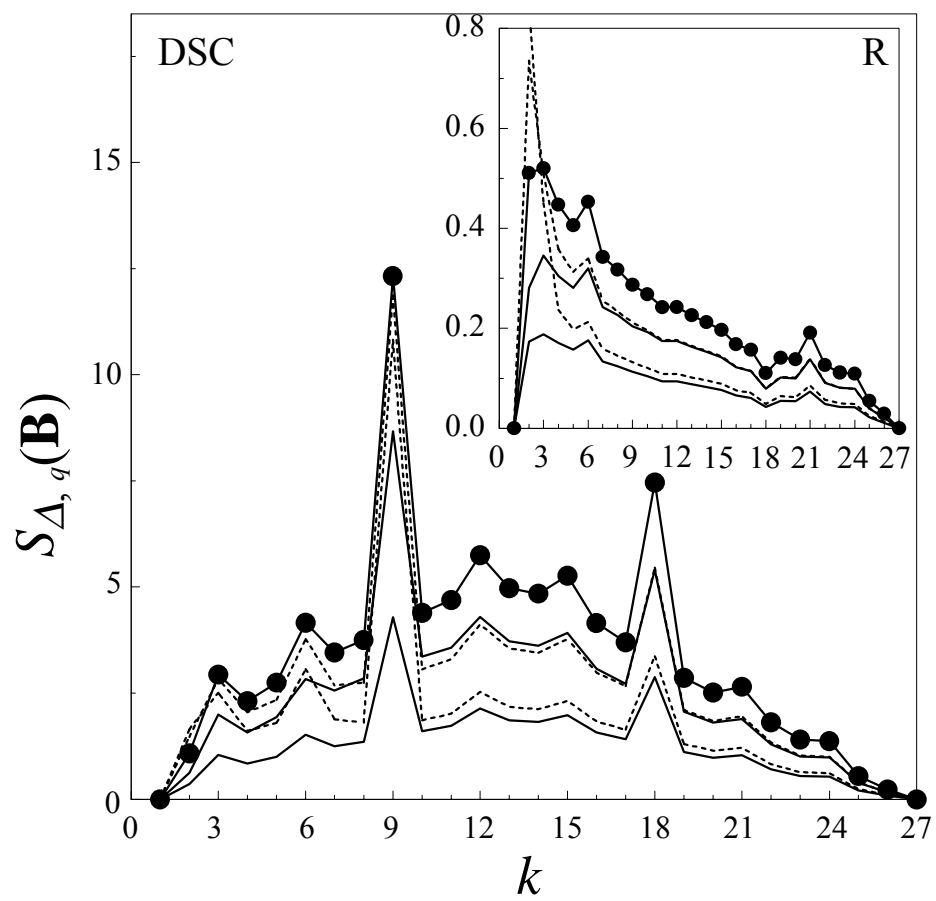


Fig. 3a

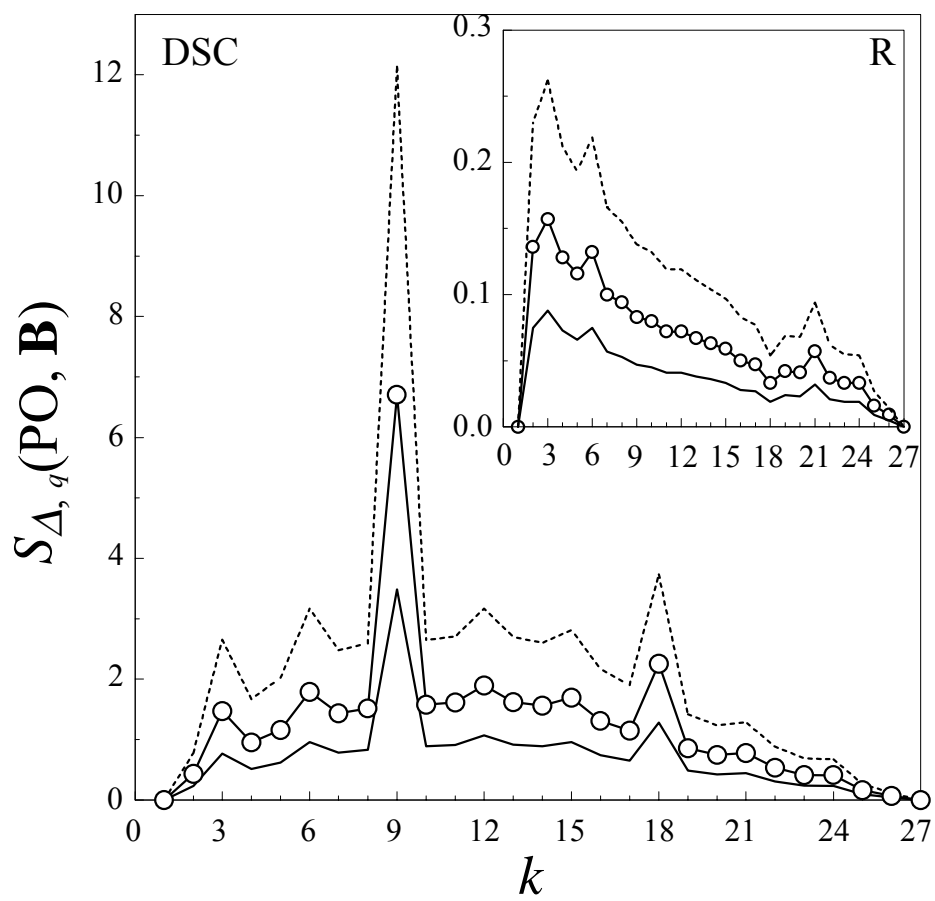


Fig. 3b

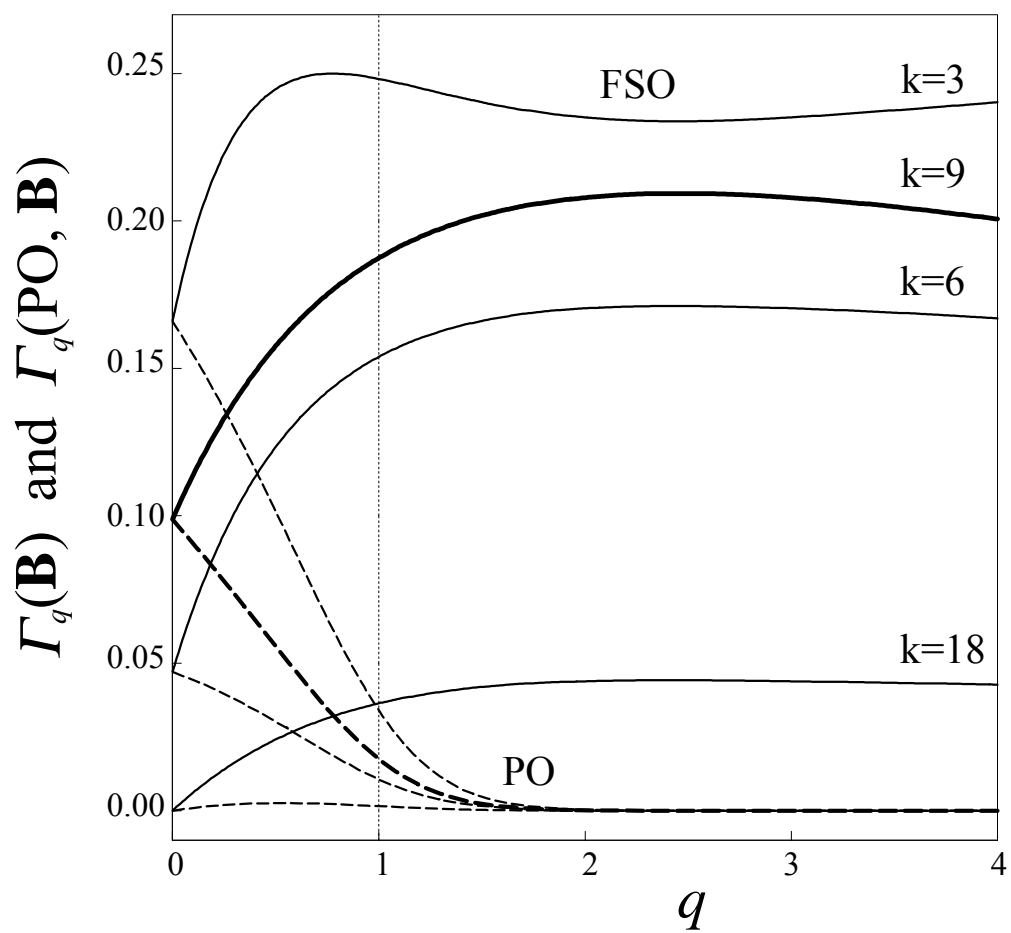


Fig. 4a

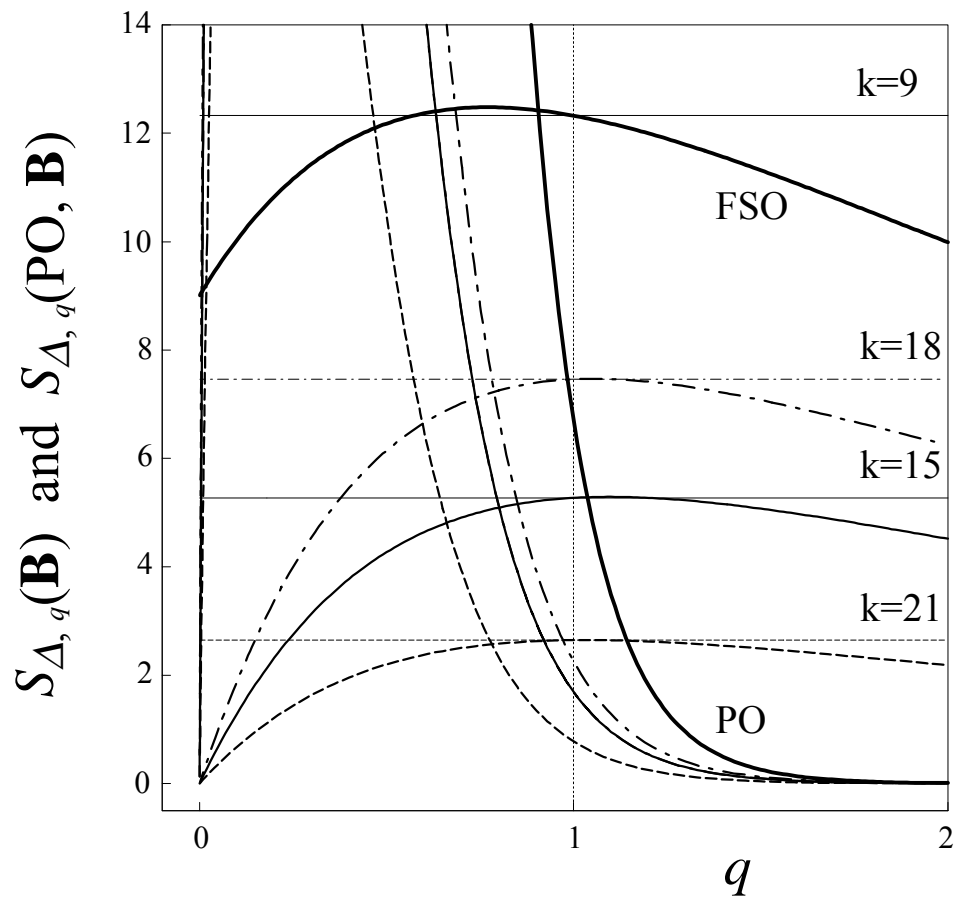


Fig. 4b

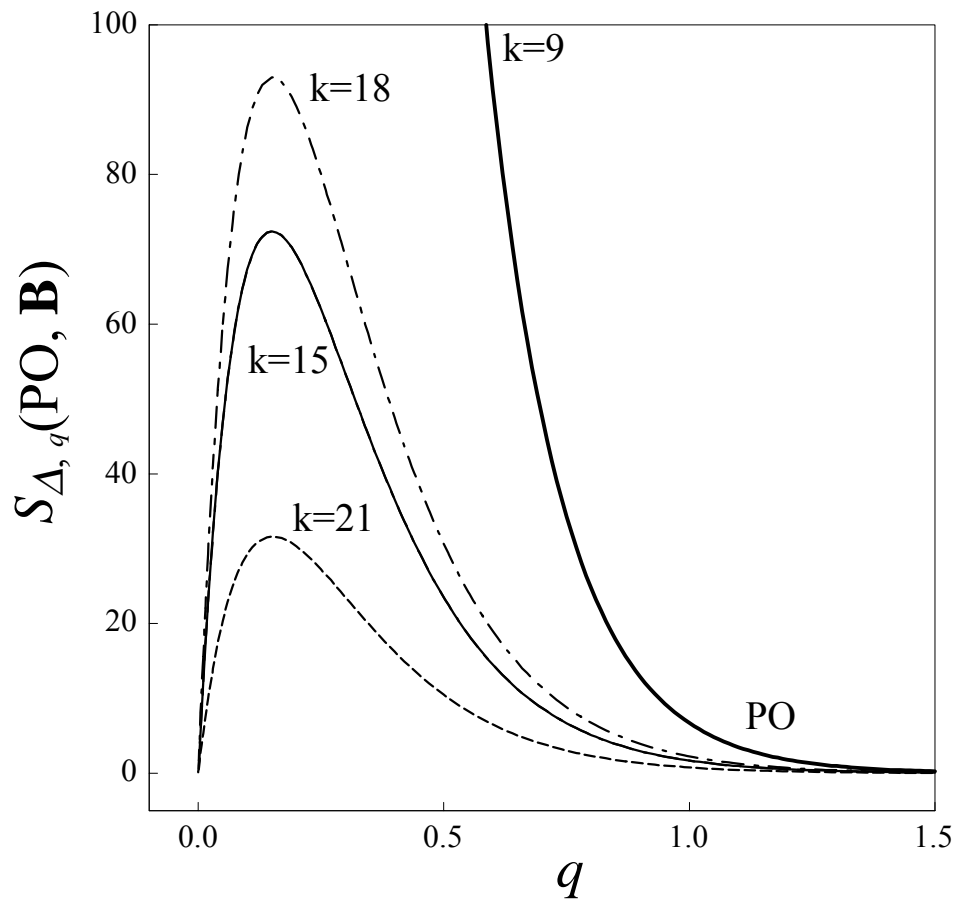


Fig. 4c